THE JOURNAL OF BIOLOGICAL CHEMISTRY
Vol. 277, No. 33, Issue of August 16, pp. 29832–29839, 2002
Printed in U.S.A.

Human ING1 Proteins Differentially Regulate Histone Acetylation*

Received for publication, January 8, 2002
Published, JBC Papers in Press, May 15, 2002, DOI 10.1074/jbc.M200197200

Diego Vieyra,[a,b,c] Robbie Loewith,[a,b,d] Michelle Scott,[a,b,d,e] Paul Bonnefin,[a] Francois-Michel Boisvert,[a,d] Parneet Cheema,[a] Svitlana Pastyryeva,[a] Maria Meijer,[a] Randal N. Johnston,[a,f] David P. Bazett-Jones,[g] Steven McMahon,[h,i] Michael D. Cole,[j] Dallan Young,[a] and Karl Riabowol[a,k]

From the [a]Departments of Biochemistry and Molecular Biology and Oncology, University of Calgary, Calgary, Alberta T2N 4N1, Canada, [f]Genome Prairie, Calgary, Alberta T2L 2K7, Canada, the [g]Programme in Cell Biology, The Hospital for Sick Children, Toronto, Ontario M5G 1X8, Canada, the [h]Molecular Genetics Program, The Wistar Institute, Philadelphia, Pennsylvania 19104, and the [j]Department of Molecular Biology, Princeton University. Princeton, New Jersey 08544-1014

ING1 proteins are nuclear, growth inhibitory, and regulate apoptosis in different experimental systems. Here we show that similar to their yeast homologs, human ING1 proteins interact with proteins associated with histone acetyltransferase (HAT) activity, such as TRRAP, PCAF, CBP, and p300. Human ING1 immunocomplexes contain HAT activity, and overexpression of $p33^{ING1b}$, but not of $p47^{ING1a}$, induces hyperacetylation of histones H3 and H4, *in vitro* and *in vivo* at the single cell level. $p47^{ING1a}$ inhibits histone acetylation *in vitro* and *in vivo* and binds the histone deacetylase HDAC1. Finally, we present evidence indicating that $p33^{ING1b}$ affects the degree of physical association between proliferating cell nuclear antigen (PCNA) and p300, an association that has been proposed to link DNA repair to chromatin remodeling. Together with the finding that human ING1 proteins bind PCNA in a DNA damage-dependent manner, these data suggest that ING1 proteins provide a direct linkage between DNA repair, apoptosis, and chromatin remodeling via multiple HAT·ING1·PCNA protein complexes.

The ING1 candidate tumor suppressor gene expresses a family of alternatively spliced mRNAs encoding proteins that localize to the nucleus and that are growth inhibitory (1–4). The locus of ING1 maps to chromosome 13q33–34 (5), a site frequently associated with loss of heterozygosity in several types of cancers (6, 7). In human cells, $p47^{ING1a}$ and $p33^{ING1b}$ are the major ING1 splicing isoforms expressed (8), and $p33^{ING1b}$ is the most intensively characterized isoform to date. Suppression of $p33^{ING1b}$ expression promotes focus formation and growth *in vitro*, and tumor formation *in vivo*, while ectopic overexpression of this protein was shown to block cell cycle progression by arresting transfected cells at G_1 of the cell cycle (2, 4). Clinical data have shown that reduced levels of $p33^{ING1b}$ are seen in primary breast tumors (9), lymphoid malignancies (10), testis (11), and squamous cell cancers (12, 13), consistent with ING1 acting as a class 2 tumor suppressor (14). $p33^{ING1b}$ also displays properties of a regulator of apoptosis in different experimental systems (15–20). Both the apoptotic and cell cycle regulatory properties of $p33^{ING1b}$ may involve the tumor suppressor p53, with which $p33^{ING1b}$ and the closely related $p33^{ING2}$ were found to be capable of physically and/or functionally interacting (16, 20–22). Finally, we have recently reported that $p33^{ING1b}$ was able to bind to PCNA in a DNA damage-inducible manner that was directly linked to the ability of $p33^{ING1b}$ to induce apoptosis (17).

Recent studies suggest that human ING1 proteins might be involved in chromatin remodeling functions via physical association with both histone acetyltransferases (HATs)[1] and histone deacetylases (HDACs). We initially reported that an ING1 yeast homolog protein, Yng-2, was able to interact with Tra1 (23), a protein that is part of HAT complexes such as SAGA and NuA4 (24, 25). Recently, while Yng-2 was shown to be essential for a Nu4A-mediated HAT activity controlling cell proliferation (26, 27), the human $p33^{ING1b}$ was found to be functionally and physically linked to HDAC1 (28, 29). Despite these observations, neither the biochemical role(s) of human ING1 proteins in HAT-related functions nor the biological significance of these functions is fully understood. Furthermore, there is no information published regarding the functions and biological properties of $p47^{ING1a}$, the other major human isoform of ING1. We have recently reported[2] that different ING1 proteins displayed isoform-dependent apoptotic properties correlated with differential binding affinity to chromatin. These observations led us to ask in the current study: (*a*) whether human ING1 proteins could physically associate with HATs in the same way as yeast Yng-2 associates with Tra1 (23); (*b*) whether human ING1 immunocomplexes were able to co-precipitate HAT activity; (*c*)

* This work was supported by grants from the Canadian Institutes of Health Research (CIHR) (to D. P. B.-J.), the Edward Mallinckrodt Foundation and the American Association for Cancer Research (to S. M.), the Alberta Cancer Board (ACB) (to R. N. J., D. P. B.-J., D. Y., and K. R.), and the CIHR and the National Cancer Institute of Canada (to D. Y. and K. R.). The costs of publication of this article were defrayed in part by the payment of page charges. This article must therefore be hereby marked "*advertisement*" in accordance with 18 U.S.C. Section 1734 solely to indicate this fact.
[b] The first three authors contributed equally to this study.
[c] Supported by CIHR, Alberta Heritage Foundation for Medical Research (AHFMR), and ACB doctoral scholarships.
[d] These authors were supported by AHFMR studentships.
[e] Supported by the National Sciences and Engineering Research Council.
[i] Special Fellow of the Leukemia Society of America.
[k] CIHR and AHFMR Scientist. To whom correspondence should be addressed: 370 Heritage Medical Research Bldg., 3330 Hospital Dr. NW, Calgary, Alberta T2N 4N1, Canada. Tel.: 403-220-8695; Fax: 403-270-0834; E-mail: karl@ucalgary.ca.

[1] The abbreviations used are: HAT, histone acetyltransferase; PCNA, proliferating cell nuclear antigen; PBS, phosphate-buffered saline; GFP, green fluorescent protein; FACS, fluorescence-activated cell sorter; DAPI, 4′,6-amidino-2-phenylindole; IP-W, immunoprecipitation-Western; FAT, factor-associated acetyltransferase; HDAC, histone deacetylase.

[2] Vieyra, D., Toyama, T., Hara, Y., Boland, D., Johnston, R., and Riabowol, K. (2002) *Cancer Res.* **62,** in press.

whether different human ING1 isoforms would display differential HAT/HDAC properties correlated with their differential binding to HATs, and if so (*d*) whether these ING1 biochemical functions correlated with any apoptotic effect. Finally, since $p33^{ING1b}$ was reported to be involved in UV-induced damage responses (30), and we observed an UV-dependent physical interaction between ING1 proteins and PCNA (17), which was functionally relevant for UV-mediated apoptosis (17), we asked (*e*) whether ING1 proteins could alter the recently noted association between p300 and PCNA (31), an association that suggests a linkage exists between the repair of UV-damaged DNA and the global regulation of gene expression through histone acetylation (31).

To address these questions, we have characterized the molecular, biochemical, and biological properties of the two major human ING1 isoforms, $p47^{ING1a}$ and $p33^{ING1b}$, regarding their roles in functions related to the acetylation of chromatin. We present evidence indicating that similar to yeast ING1 immunocomplexes (23), human ING1 immunocomplexes co-precipitate HAT activity. We show that ING1 proteins physically interact with proteins present in complexes containing HAT activity such as CBP, PCAF, p300, and TRRAP. TRRAP, the human homolog of yeast Tra1 which interacts with Yng-2 (23), is a 434-kDa c-Myc-interacting nuclear protein that binds the c-Myc amino terminus and the E2F-1 transactivation domain and is an essential co-factor for c-Myc and adenovirus E1A-mediated oncogenic transformation (32); TRRAP recruits at least one HAT, hGCN5, to a complex containing c-Myc (24, 33).

These physical associations, HAT activities and biological properties associated with ING1 proteins, were found in the present study to be isoform-dependent. Overexpression of $p33^{ING1b}$, but not $p47^{ING1a}$, induced apoptosis and hyperacetylation of histones H3 and H4 both *in vitro* and *in vivo* at a single cell level. Conversely, ectopic up-regulation of $p47^{ING1a}$ resulted in a decrease of the levels of histone acetylation *in vitro* and *in vivo* accompanied by no changes in the percentage of apoptosis compared with the empty vector control. In agreement with this observation, we have found that $p47^{ING1a}$ avidly binds to the histone deacetylase HDAC1. Finally, we present evidence indicating that $p33^{ING1b}$ affects the degree of physical association between PCNA and p300, an association that has been proposed to link DNA repair to chromatin remodeling functions (31).

EXPERIMENTAL PROCEDURES

Cell Culture—Primary normal human diploid fibroblasts (Hs68; ATCC CRL#1635) and established human glioblastoma cells (SNB19; ATCC CRL#2219) were used in these studies, since Hs68 cells are phenotypically normal, and SNB19 cells have relatively high levels of endogenous ING1 proteins. For blocking HDAC activity (Fig. 6) a bolus of 5 mM sodium butyrate was added to the media for 24 h. For UV-irradiation experiments (Fig. 3), cell plates were rinsed thrice with PBS and exposed to UV (25 J/m^2) as described previously (17, 18).

Plasmids and Transfections—ING1 cDNAs (8) were subcloned into pCI vector (Promega). All experiments included parallel controls of cells transfected with green fluorescent protein (GFP) (CLONTECH) expression plasmids to determine the proportion of transfected cells. Cells were electroporated as described previously (17, 18). For Western blots (Fig. 6), cells were co-transfected with ING1 and GFP expression constructs at an ING1:GFP plasmid ratio of 4:1.

Antibodies, Immunoprecipitation, and Western Blot Assays—ING1 polyclonal rabbit antibodies (2, 34), the four mouse CAb ING1 monoclonals (35), and the c-Fos mouse monoclonal antibodies (36) have been characterized previously. We also used rabbit polyclonal anti-acetyllysine (New England Biolabs #9441S and Upstate Biotech #06-933), anti-CBP (Santa Cruz #sc-583), anti-PCAF (Santa Cruz #sc-6301), anti-p300 (Santa Cruz #sc-584), anti-TRRAP (33), and goat polyclonal anti-GCN5 (Santa Cruz #sc-6302) antibodies. Both rabbit and mouse anti-ING1 antibodies were raised against a GST-ING1 fusion protein and both recognize native and denatured forms of $p33^{ING1b}$ and $p47^{ING1a}$, as well as the truncated $p24^{ING1c}$ isoform (8, 35). The ING1 monoclonals were not frozen before use. Immunoprecipitations used 5 μl of polyclonal or affinity-purified monoclonal anti-ING1 antibodies or 50 μl of concentrated hybridoma supernatant. Western blots were done with 1:500 to 1:1000 dilutions of polyclonal or affinity-purified monoclonal antibodies or with monoclonal hybridoma supernatants diluted 1:1 with the same buffer used to dilute polyclonal antibodies. Horseradish peroxidase-conjugated secondary antibodies against the appropriate species that were used for Western blotting were from Amersham Biosciences and were all used at 1:1000. Acetylated histones were visualized using antibodies recognizing either diacetylated histone H3 (Upstate #06-599) or histone H4 acetylated on lysine 5 (Upstate #06-759). For assays shown in Fig. 6, cells were co-transfected with ING1 and GFP expression constructs. 48 h later, green cells were sorted by FACS and harvested for Western blot assays.

Microscopy and Microinjection of Somatic Cells—Cells were cultured, microinjected, fixed, and mounted as described (17, 37). Acetylated histones were visualized using the above-mentioned antibodies according to the supplier's recommendations. After washing, cells were incubated with the secondary antibodies goat anti-rabbit IgG (Cy3, Chemicon) or goat anti-mouse IgG (Alexa 488, Cedarlane or Cy5, Chemicon). After rinsing, the samples were mounted in 1 μg/ml paraphenylenediamine in PBS, 90% glycerol that also contained the DNA-specific dye DAPI at 1 μg/ml. Imaging was performed using a 14-bit cooled CCD camera (Princeton Instruments) mounted on a Leica DMRE immunofluorescence microscope. For signal density quantitation, the nuclear signal of acetylated histones was integrated for injected and non-injected cells, using ERGOvista v4.4 software.

FACS Analysis and Cell Sorting—For analysis of apoptosis, cells electroporated with ING1 expression constructs were harvested at 48 h, fixed in 70% ethanol/PBS, on ice for 1 h after which they were subjected to analysis or were kept at −20 °C for no more than 1 week. Before analysis using a Becton Dickinson FACS scanner, ethanol was removed, and cells were resuspended in PBS for 10 min, after which they were pelleted, the PBS was removed, and the cells were treated with staining solution (5 μg/ml propidium iodide (Sigma), 1 mg/ml RNase A (Roche Molecular Biochemicals) in PBS). Analyses of flow cytometry data were done using ModFit software (Verity Inc.). For preparation of lysates from ING1/GFP transfectants (Fig. 6), electroporated cells were harvested at 48 h, rinsed in PBS, and kept alive in media containing 1% serum on ice until being sorted by FACS. Green cells (positive transfectants) were collected, harvested, and their lysates were used for Western blot experiments.

RESULTS

ING1 Proteins Associate with Specific HATs—Based on our finding that a yeast ING1 homolog physically interacted with Tra1 (23), we asked whether human ING1 proteins would be able to bind to TRRAP, the human homolog of Tra1, as well as to other proteins of the GNAT and MYST HAT superfamilies (24, 32). To test this hypothesis, we made use of immunoprecipitation-Western (IP-W) assays. As shown in Fig. 1, *A–D*, immunoprecipitation of endogenous ING1 proteins from lysates of SNB19 cells co-precipitated several HATs, including TRRAP, PCAF, and CBP. Although we were able to find a weak physical association between ING1 proteins and PCAF, which is a member of the hGNC5 family of HATs (24), we were unable to find any interaction between ING1 proteins and hGCN5 (Fig. 1*C*). To confirm that the interaction between ING1 and one of the HAT complex proteins was specific, we tested whether anti-CBP, but not rabbit preimmune control immunoprecipitates, was able to co-immunoprecipitate ING1 proteins. As shown in Fig. 1*E*, a weak but reproducible band in the anti-CBP lane corroborated the idea that the ING1-CBP interaction was specific. Similar results were obtained in primary fibroblast cells (data not shown). Because of this apparently weak association between CBP and ING1 proteins, we wanted to test whether this interaction was increased upon ectopic up-regulation of these proteins. For this purpose, we performed IP-W assays on lysates of primary human fibroblasts overexpressing these proteins upon co-transfection of constructs encoding CBP and either $p47^{ING1a}$, $p33^{ING1b}$, or empty expression vector (indicated as *a*, *b*, and *v* in Fig. 2). IP-W assays showed that while both ING1 isoforms bound CBP, $p33^{ING1b}$ appeared

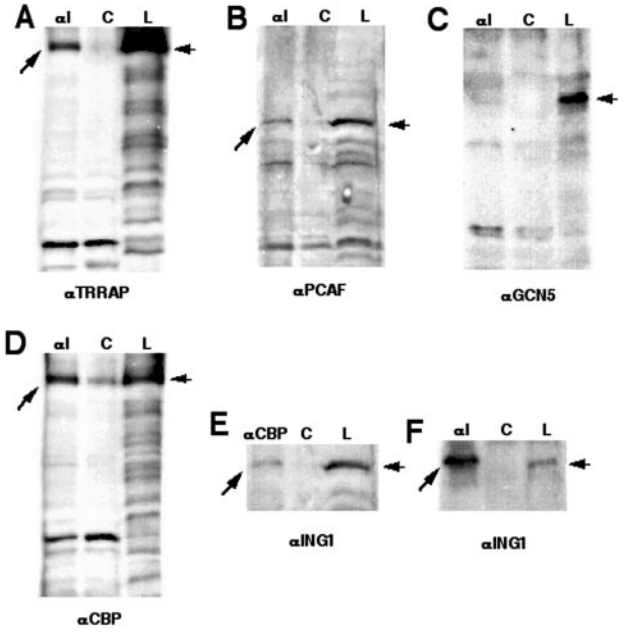

FIG. 1. **HAT proteins bind ING1 proteins.** SNB19 cells (5×10^6 per IP) were harvested under non-denaturing conditions, and lysates were immunoprecipitated with a mixture of mouse anti-ING1 monoclonal antibodies (indicated as *αI* in *A–D*), anti-CBP (indicated as *αCBP* in *E*), or anti-FOS (used as control and indicated as "*C*") antibodies. Before immunoprecipitations, aliquots of each lysate (*L*) were taken to be used as positive controls. Equal amounts of these immunoprecipitates and the aliquots of lysates were separated by 7% (for proteins >75 kDa) or 15% (for proteins <75 kDa) PAGE, transferred to nitrocellulose, and blotted with the antibodies indicated at the *bottom* of each panel. *Arrows* indicate the expected sizes of the proteins recognized by the blotting antibodies mentioned at the bottom of each panel.

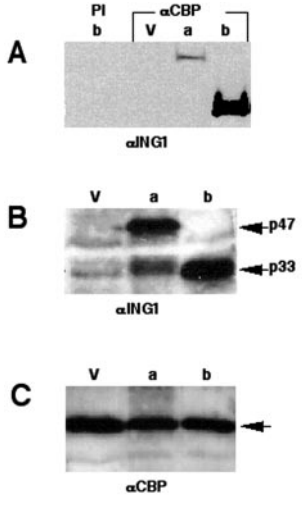

FIG. 2. **$p47^{ING1a}$ and $p33^{ING1b}$ interact with CBP.** Hs68 cells transfected with empty vector as a negative control (*V*), $p47^{ING1a}$ (*a*), or $p33^{ING1b}$ (*b*) expression constructs were harvested under non-denaturing conditions, and their lysates were immunoprecipitated with either preimmune sera (*PI*) or with anti-CBP antibodies. These immunoprecipitates were separated by PAGE, transferred to nitrocellulose, and blotted with anti-ING1 antibodies as shown in *A*. Aliquots of the same lysates used in *A* were electrophoresed, and separated proteins were assayed by Western blotting to test for the levels of ING1 proteins (*B*) or CBP (*C*). Note that although both ING1 proteins bind to CBP, $p33^{ING1b}$ binds considerably more avidly.

to bind it much more avidly than $p47^{ING1a}$ (Fig. 2*A*). To confirm that the difference in the affinity of ING1 isoforms by CBP was not due to different expression levels of these proteins (*i.e.* as a consequence of differences in the efficiencies of transfection), we performed anti-ING1 (Fig. 2*B*) and anti-CBP (Fig. 2*C*)

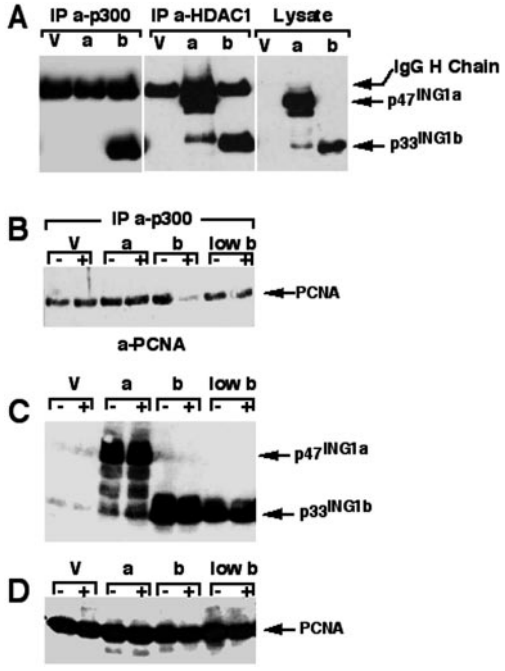

FIG. 3. **Differential binding of ING1 isoforms to HAT and HDAC proteins.** Hs68 cells transfected with empty vector (*V*), $p47^{ING1a}$ (*a*), or $p33^{ING1b}$ (*b*) expression constructs were harvested under non-denaturing conditions, and resulting lysates were immunoprecipitated with anti-p300 or anti-HDAC1 antibodies. Aliquots of each lysate were isolated and blotted in parallel and served as a positive control for ING1 isoform expression and blotting efficiency as shown in the *third panel* of *A* (*Lysate*). Equal amounts of these immunoprecipitates and the aliquots of lysates were separated by PAGE, transferred to nitrocellulose, and blotted with anti-ING1 (*A*) or anti-PCNA (*B*) antibodies. Signs "+" and "−" in *B* refer to whether ING1 transfectants were UV-irradiated with 25 J/m^2 (+), which is known to induce an interaction between $p33^{ING1b}$ and PCNA (17), or not (−). In *B*, "*low b*" indicates cells transfected with 20% (2 μg) of the amount of ING1b expression constructs normally used, which led to lower levels of $p33^{ING1b}$ than regular ING1b transfectants (indicated simply as *b* and see *panel C*). *C* and *D* show control Western blots of lysates, which verify expression of the transfected constructs. Note that while HDAC1 binds to both ING1 proteins, p300 binds strongly to $p33^{ING1b}$ (*A*). Also note that overexpression of $p33^{ING1b}$ decreases the amount of PCNA recovered in p300 immunoprecipitates after UV irradiation (*B*), suggesting that high levels of $p33^{ING1b}$ might physically interfere with the p300-PCNA interaction.

Western assays on the total lysates used in Fig. 2*A*. As shown in Fig. 2, *B* and *C*, the level of CBP was very similar in the three lanes, and the levels of both $p33^{ING1b}$ and $p47^{ING1a}$ were also similar, confirming that the difference in the binding affinity of ING1 isoforms for CBP was not an artifact due to variable transfection or expression efficiencies.

ING1 Proteins Bind to p300 and PCNA, Regulating the Association between These Proteins in an UV-inducible Manner—Since ING1 proteins were able to bind to CBP (Figs. 1 and 2) and to PCNA (17), CBP is closely related to p300 (38–40, 45), and a recent report has indicated that p300 was able to bind PCNA through an unidentified nuclear protein (31), we asked whether $p47^{ING1a}$ and/or $p33^{ING1b}$ bound p300, and if so: (*a*) whether ING1 proteins would be present in the same complex as p300 and PCNA and (*b*) whether altering the levels of cellular ING1 proteins would affect the interaction between p300 and PCNA. To address the first point, we performed p300 and ING1 IP-W assays on lysates of primary human fibroblasts transiently transfected with ING1 expression constructs. As shown in the *leftmost panel* of Fig. 3*A*, we found that ING1 proteins bound p300 in an isoform-dependent manner. Anti-p300 immunoprecipitates contained $p33^{ING1b}$, but not $p47^{ING1a}$. Since it was recently reported that $p33^{ING1b}$ was able

to bind to HDAC1 (28, 29), we used anti-HDAC1 antibodies as positive control for our IP-W assay. Data shown in the *second panel* of Fig. 3*A* confirmed the reported association between $p33^{ING1b}$ and HDAC1 in our normal human fibroblast model and demonstrated a novel and robust physical interaction between $p47^{ING1a}$ and HDAC1.

To test whether increased levels of $p33^{ING1b}$ could affect the formation of p300·PCNA complexes (31), we followed a similar strategy. Since $p33^{ING1b}$ and PCNA associate in an UV-inducible manner (17), we tested for the presence of PCNA and ING1 proteins in anti-p300 immunoprecipitates from lysates of ING1 transient transfectants subjected to UV-irradiation (Fig. 3, *B–D*). Fig. 3*C* shows that ING1 transfection resulted in the expected overexpression of $p47^{ING1a}$ and $p33^{ING1b}$ in the absence and in the presence of UV. Fig. 3*D* shows that PCNA levels were not altered appreciably under these conditions. Aliquots of the same cell lysates blotted in Fig. 3, *C* and *D*, were immunoprecipitated with anti-p300 antibodies, and immunoprecipitates were blotted with anti-PCNA antibodies (Fig. 3*B*). As shown in Fig. 3*B*, p300 and PCNA were found together in complexes that were not altered by UV alone (lanes with vector transfected) as reported previously (31). However, while high levels of $p47^{ING1a}$ did not appreciably alter the amount of PCNA complexed with p300, and low levels of $p33^{ING1b}$ had a modest effect, overexpression of higher levels of $p33^{ING1b}$ selectively interfered with the p300-PCNA interaction following UV exposure (compare *lane b−* to *lane b+* in Fig. 3*B*).

ING1 Immunoprecipitates Contain HAT Activity—Since human ING1 proteins interacted with HATs (Figs. 1–3), and yeast ING1 immunoprecipitates contained HAT activity (23), we asked whether human ING1 immunoprecipitates contained HAT activity. For this purpose, we made use of an *in vitro* HAT assay in which anti-ING1 immunoprecipitates were incubated with purified histones in the presence of [^{3}H]acetyl-coenzyme A, after which the level of histone acetylation was determined by polyacrylamide gel electrophoresis (PAGE) followed by fluorography. This activity was assayed on anti-ING1 immunoprecipitates from fibroblast lysates of cells that were untransfected (Fig. 4*A*) or transfected (Fig. 4, *B–D*) with ING1 expression constructs encoding $p33^{ING1b}$ and $p47^{ING1a}$ (indicated as *b* and *a*, respectively, in Fig. 4, *B–D*). Fig. 4*A*, therefore, shows the level of HAT activity associated with endogenous ING1 proteins (non-transfected cells), while Fig. 4, *B* and *D*, depict the HAT activity associated with ectopically up-regulated ING1 isoforms. Fig. 4*B* represents the HAT activity associated with anti-ING1 immunoprecipitates, and Fig. 4*D* represents the HAT activity of total lysates (non-immunoprecipitated lysates) of ING1 transfectants containing equal amounts of protein. Fig. 4*C* is a Coomassie gel of samples from Fig. 4*B*. As shown in these figures, anti-ING1 antibodies (αI) precipitated abundant HAT activity, whereas preimmune sera did not. The autoradiograph shown in Fig. 4*A* was overexposed to demonstrate that even though Fos has been reported to bind to CBP (41), Fos antibodies precipitated less than 10% of the HAT activity seen in ING1 immunoprecipitates, consistent with ING1 isoforms associating with multiple HAT complexes. This HAT activity was ING1-specific, since blocking the anti-ING1 antibodies by preincubation with a GST-ING1 fusion protein markedly decreased this co-precipitated HAT activity (Fig. 4*A*, compare *αI* with *αI+P*).

Different ING1 Isoforms Are in Complexes Displaying Different Histone Acetylation Properties—Since ING1 isoforms differentially interacted with different HATs (Figs. 2 and 3), we asked whether different isoforms of ING1 co-precipitated different HAT activities, and if so, whether it was possible to alter the amount of co-precipitable HAT activity by ectopically increasing the protein levels of these isoforms. For this purpose,

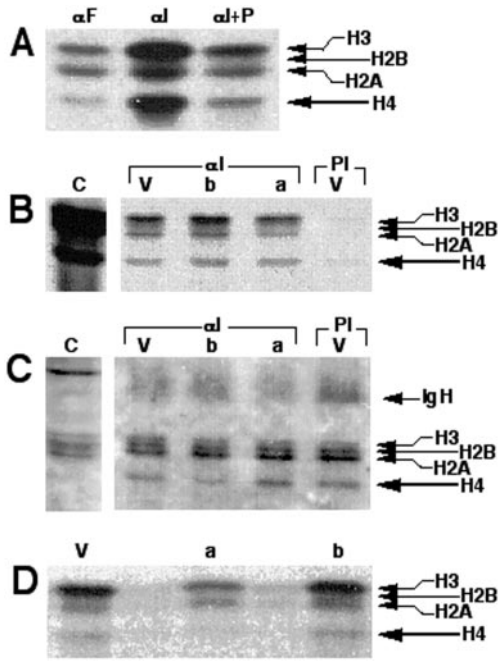

FIG. 4. **ING1 immunoprecipitates contain histone acetyltransferase activity as estimated by *in vitro* HAT assays.** Anti-ING1 (*αI*), anti-Fos (*αF*), and preimmune (*PI*) immunoprecipitates, as well as lysates containing proven HAT activity (*C*), were incubated with purified histones in the presence of [^{3}H]acetyl-coenzyme A, after which the level of histone acetylation was determined by PAGE of the reaction samples followed by fluorography. *A* shows the level of HAT activity associated with endogenous ING1 proteins (non-transfected cells). *B* shows the HAT activity associated with immunoprecipitates of cells transfected with empty vector as a negative control (*V*), $p33^{ING1b}$ (*b*), or $p47^{ING1a}$ (*a*). *C* shows a Coomassie Blue-stained gel of samples from *B* and serves to verify equal protein loading of the gel. *D* represents the HAT activity present in total lysates of the ING1 transfectants of *B*. Note that the HAT activity immunoprecipitated by anti-ING1 antibodies is ING1-specific, since preblocked antibodies (*αI+P* in *A*) significantly reduced the amount of HAT activity immunoprecipitated. Note also that this ING1-dependent HAT activity was isoform-dependent (compare the intensities of bands for *lanes a* and *b* on *B* and *D*).

human fibroblast cells were transfected with empty vector or with expression constructs encoding $p33^{ING1b}$ or $p47^{ING1a}$ (indicated as *v*, *b*, and *a*, respectively, in Fig. 4, *B–D*). As shown in Fig. 4*B*, overexpression of $p33^{ING1b}$ allowed recovery of slightly greater amounts of HAT activity in anti-ING1 immunoprecipitates compared with cells transfected with empty vector. In contrast, overexpression of $p47^{ING1a}$ reduced the recovery of anti-ING1-associated HAT activity from cell lysates (Fig. 4*B*). This effect might be due to overexpression of $p47^{ING1a}$ acting to competitively inhibit the binding of endogenous $p33^{ING1b}$ either to HAT complexes or to ING1 antibodies. As shown in Fig. 4*C*, a Coomassie staining assay for histone substrate proteins of the autoradiogram of Fig. 4*B* confirmed that these differences in the amounts of HAT activity precipitated by the different ING1 isoforms were not due to differences in the amounts of substrate during the HAT assays. As shown in Fig. 4*B*, similar results were obtained by quantitation of HAT activity from total lysates of ING1 transfectants. These data are consistent with data of Fig. 1 and support the idea that ING1 proteins contribute to the regulation of multiple HAT complexes. The magnitudes of these differences, as estimated by scanning densitometry, were on average a 60% increase and a 45% decrease for ING1b- and ING1a-transfected cells, respectively, but these relatively modest changes are most likely due to low transfection efficiencies of human fibroblasts that typically range from 10 to 40%.

ING1 Proteins Regulate Acetylation of Histones H3 and H4 in

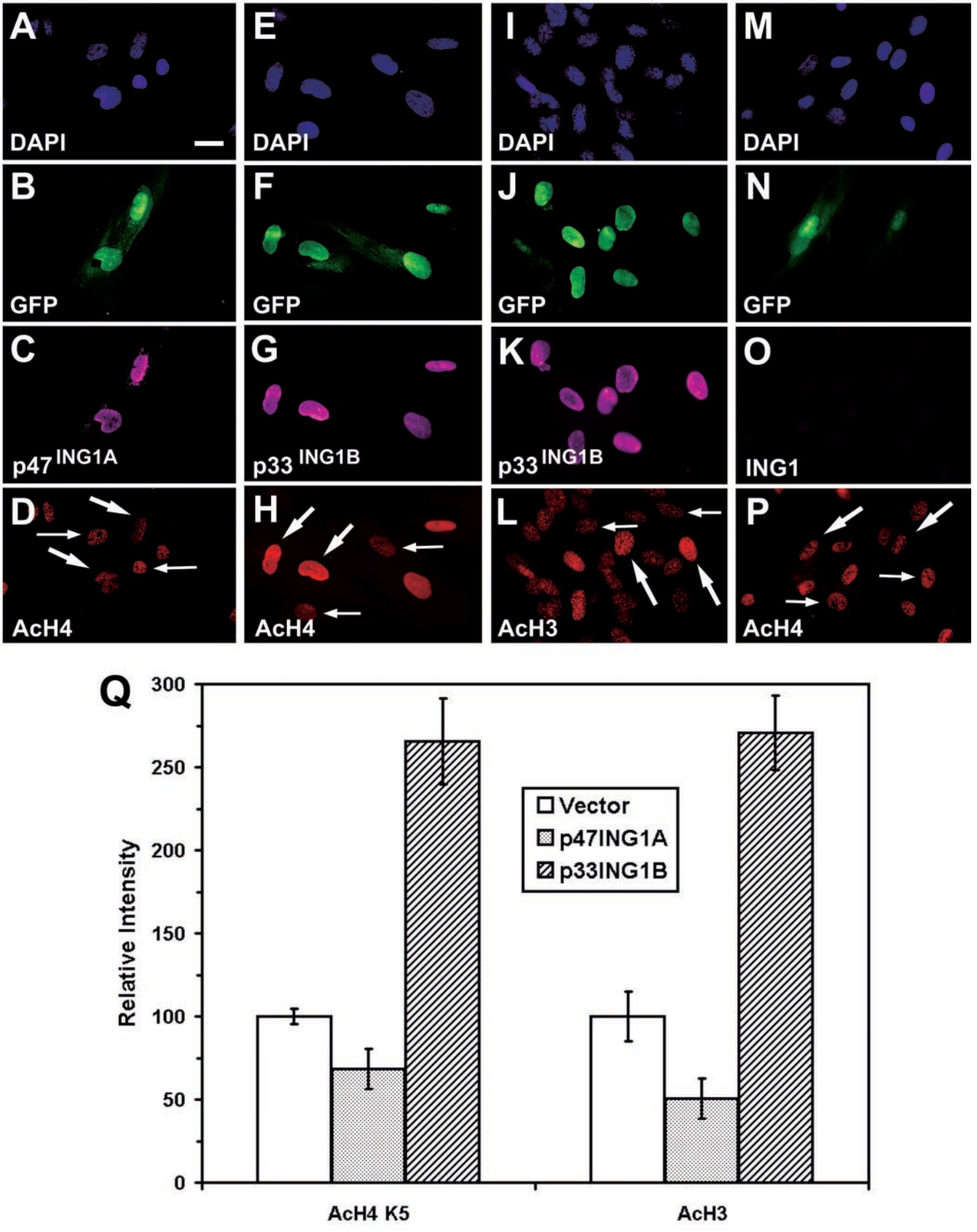

FIG. 5. **ING1 isoforms regulate the acetylation of histones H3 and H4 *in vivo*.** Hs68 cells were microinjected in the nucleus with a mixture of GFP (microinjection marker) and ING1 expression constructs. 24 h later these cells were fixed and processed for immunofluorescence microscopy. Each column of figures represents the same field of cells showing fluorescence after staining for DNA (indicated as *DAPI*), successful microinjection (*GFP*), ING1 expression, and acetylated histone H3 (*AcH3*) or H4 (*AcH4*). *A–D* show cells injected with ING1a plus GFP; *E–L* show cells that were injected with ING1b plus GFP; and *M–P* represent cells that were injected with GFP plus empty vector (control). *Thick arrows* highlight injected cells, while *thin arrows* identify uninjected cells (which represent the immunofluorescence background). The *bar* in *A* represents

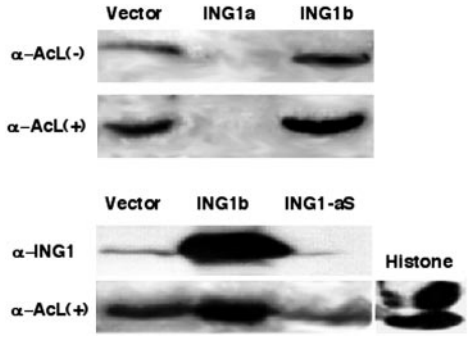

FIG. 6. **ING1-induced changes in histone acetylation.** Hs68 cells were co-electroporated with 20 μg of plasmid DNA per 5×10^6 cells (electroporation conditions: 250 V, 960 microfarads, and t values of 18–22), harvested 48 h after electroporation, sorted by FACS, lysed; and lysates were electrophoresed, transferred, and blotted with the antibodies indicated. The *first two panels* show lysates from cells transfected with vector (as a negative control), $p47^{ING1a}$ or $p33^{ING1b}$ expression constructs, and grown in the absence (−) or presence (+) of the HDAC inhibitor sodium butyrate. The *panel* marked *Histone* represents a purified histone fraction run in parallel where the fastest migrating band represents histone H4.

Vivo—Since in transfection experiments only a subset of cells typically takes up DNA, we followed a needle microinjection approach combined with immunofluorescence studies to visualize, at the individual cell level, changes in acetylation of histones upon ectopic up-regulation of ING1 isoforms. Fig. 5 shows four fields of human fibroblasts coinjected with a GFP expression construct (used as a positive coinjection marker) and either $p47^{ING1a}$ (Fig. 5, *A–D*), $p33^{ING1b}$ (Fig. 5, *E–L*) or empty vector (Fig. 5, *M–P*). 24 h after injection, cells were fixed and stained with DAPI to identify nuclei and immunostained to detect both ING1 expression and either acetylation of histone H4 (Fig. 5, *A–H* and *M–P*) or histone H3 (Fig. 5, *I–L*). As shown in Fig. 5, *E–L*, cells microinjected with $p33^{ING1b}$ expression constructs (*thick arrows*) displayed increased staining for acetylated histones H4 and H3 compared with both uninjected cells (*thin arrows*) and cells injected with empty vector (*thick arrows* in Fig. 5, *M–P*). In contrast, cells microinjected with $p47^{ING1a}$ constructs (*thick arrows* in Fig. 5, *A–D*) showed decreased staining for acetylated H4 compared with either uninjected cells (*thin arrows* in Fig. 5, *A–D*) or cells injected with empty vector (*thick arrows* in Fig. 5, *M–P*). The statistical analysis of these fluorescent intensities is summarized in Fig. 5*Q*, which shows the means of staining intensities of ten randomly chosen injected cells for each ING1 expression construct. Overexpression of $p33^{ING1b}$ increased the fluorescent intensity associated with acetylation of histone H3 and H4 by 2.7 and 2.8-fold, respectively, while $p47^{ING1a}$ reduced these intensities by ~0.5-fold compared with cells injected with empty vector. Although we do not consider these values entirely quantitative due to the constraints of immunofluorescence and the limited number of cellss that it was practical to examine, microinjection of CBP expression constructs resulted in a relatively similar increase in acetylation compared with $p33^{ING1b}$ (~5-fold, data not shown).

Ectopic Down-regulation of $p33^{ING1b}$ Decreases the Level of Histone Acetylation—To examine the effects of altering the levels of $p33^{ING1b}$ on histone acetylation using an independent method, we electroporated Hs68 cells with a GFP expression construct together with ING1 expression constructs, after

TABLE I
Effect of ING1 overexpression on histone H4 acetylation by three independent methods

In each case, values obtained with control vector were arbitrarily set to a value of 1. Values for HAT assays and Western blots are the average of three trials, and immunofluorescence data are the average values of 10 randomly selected individual cells.

	Relative histone H4 acetylation		
	+Vector	+p47ING1a	+p33ING1b
HAT assay (*in vitro*)	1	0.65	1.6
Immunofluorescence (*in vivo*)	1	0.65	2.7
Western blot	1	0.11	2.4

which positive transfected cells were identified and sorted by FACS. These sorted cells constituted the starting material for Western blots (biochemical studies) and apoptosis assays (biological studies). As shown in Fig. 6, Western blot assays performed on total lysates of sorted ING1 transfectants showed that ectopic up-regulation of $p33^{ING1b}$ increased the level of acetylated histones as judged by co-migration of purified histones. Conversely, ectopic down-regulation of $p33^{ING1b}$ reduced the level of histone acetylation in agreement with data from Figs. 4 and 5, indicating that a direct correlation between HAT activity and $p33^{ING1b}$ levels exists. These $p33^{ING1b}$-mediated HAT effects were further increased in the presence of the HDAC inhibitor sodium butyrate, suggesting that sodium butyrate might target molecules other than those activated by $p33^{ING1b}$, perhaps through inhibition of other isoforms of ING1 such as $p47^{ING1a}$, which avidly binds HDAC1. Alternatively, the inhibitor may serve to abolish the proposed HDAC-associated properties of $p33^{ING1b}$ (28, 29).

Table I compares the effects of $p47^{ING1a}$ and $p33^{ING1b}$ on histone H4 acetylation in three different independent assays. It should be noted that values given for *in vitro* HAT assays are minimal estimates of activity since not all cells take up expression constructs. Such significant and reproducible changes in global activity could have profound effects upon gene expression. The relatively greater inhibitory effect of $p47^{ING1a}$ in the Western blot assay is probably due to a higher proportion of cells expressing the construct (cells were FACS-purified), for a longer period of time (48 h *versus* 24 h in microinjection assays).

Differential Apoptotic Properties of ING1 Isoforms Correlate with ING1 Isoform-dependent Effects on HAT Functions—Consistent with previous studies reporting that increased histone acetylation can induce apoptosis (42, 43), we found that ectopic overexpression of $p33^{ING1b}$, but not $p47^{ING1a}$, induced apoptosis in our model. In contrast to experimental results from $p47^{ING1a}$ and empty vector transfectants, three independent experiments demonstrated that the FACS profiles of $p33^{ING1b}$ transfectants displayed an increased sub-G_1 peak, indicating the presence of an apoptotic component (Fig. 7). These observations were in agreement with recent[2] and previously published data (15–20) describing the presence of apoptotic DNA breaks (assayed by TUNEL (terminal deoxynucleotidyltransferase-mediated dUTP nick end labeling) and DNA-agarose gels), apoptotic nuclear morphology (assayed by chromatin staining), and increased sub-G_1 content (assayed by flow cytometry) in $p33^{ING1b}$ transfectants. Although $p47^{ING1a}$ did not induce apoptosis and does not induce, but instead inhibits HAT activity in our model, the ideal negative control to demonstrate a direct link between $p33^{ING1b}$-mediated HAT activity and

15 μm. *Q* shows a compilation of histone H3 and H4 staining data from 10 randomly selected microinjected cells in each category. The staining intensity in cells injected with GFP plus vector was set to a value of 100. Note that overexpression of $p33^{ING1b}$ visibly increased fluorescence in *H* (acetylated histone H4) and *L* (acetylated histone H3), while no changes were seen upon staining with anti-acetylated histone H2B (data not shown).

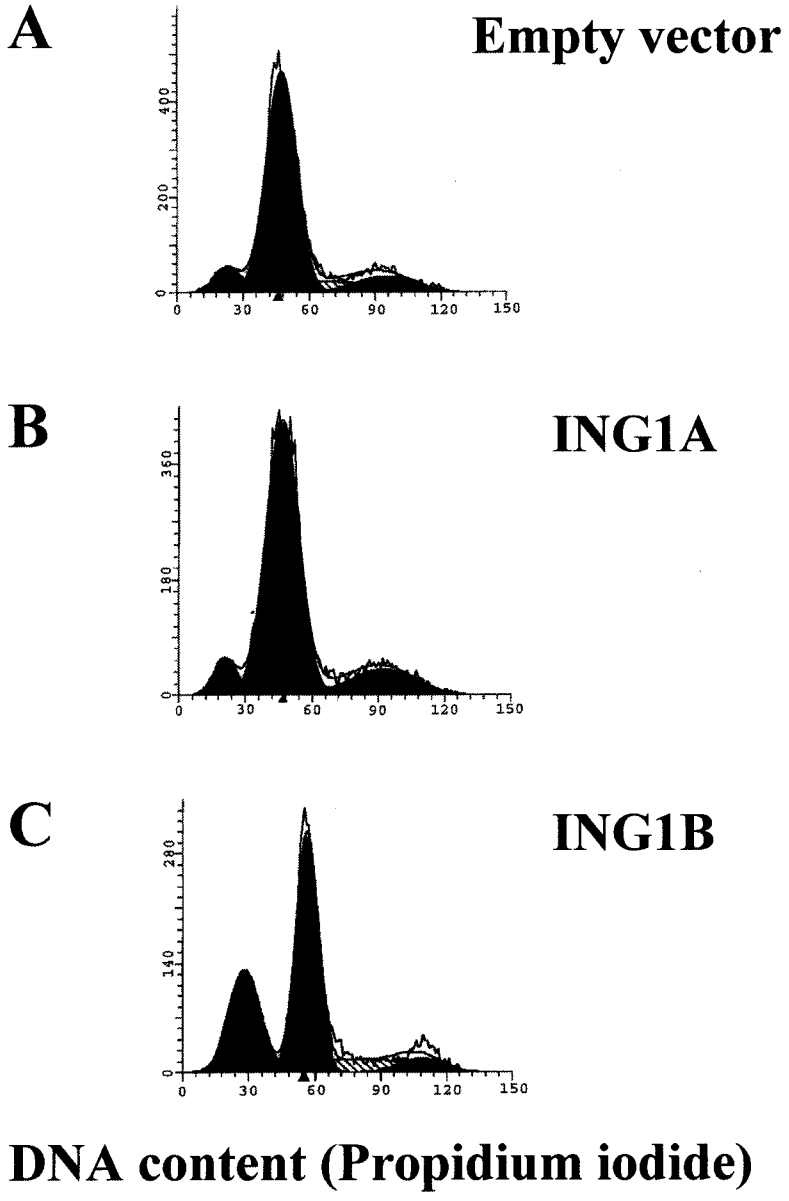

FIG. 7. **ING1 isoform-dependent apoptosis correlates with ING1-mediated HAT functions.** Hs68 cells were electroporated with empty vector (*A*), $p47^{ING1a}$ (*B*), or $p33^{ING1b}$ (*C*) expression constructs. 48 h later cells were fixed, stained for DNA content with propidium iodide, and analyzed by FACS. Data were analyzed using ModFit software. The *arrowhead* on the *abscissa* corresponds to a diploid (2N) DNA content. Note that $p33^{ING1b}$ transfectants display a significantly greater subG1 (apoptotic) component (*left* of the *arrow*) compared with the other transfectants. These data are in agreement with data from different apoptotic assays presented here and in recent previous studies.

apoptosis would have been point mutants of $p33^{ING1b}$ that do not interact with HATs. We are currently defining regions of the ING1 proteins that are responsible for such protein-protein interactions.

DISCUSSION

In this study we demonstrated that similar to yeast ING1 proteins (23), human ING1 proteins associate with HATs (Figs. 1–3), co-precipitate HAT activity (Fig. 4), and regulate the acetylation of histones *in vitro* and *in vivo* (Figs. 4–6). These properties were shown to be ING1 isoform-dependent (Figs. 4–6) and correlated with differential effects of ING1 isoforms on apoptosis (Fig. 7). Immunoprecipitation studies allowed us to identify different HAT complexes such as those containing TRRAP, CBP, p300, and PCAF as ING1-interacting complexes (Figs. 1–3), and overexpression studies supported the idea that ING1 isoforms interact directly with the HAT proteins themselves. However, this point must be confirmed by alternative approaches and is currently being addressed using purified proteins. The interaction between p300 and ING1 led us to find that ING1 proteins associated in a complex with both PCNA and p300 (Fig. 3). This association was affected by the levels ING1 in isoform-, dose-, and UV-dependent manners (Fig. 3). By means of several independent studies, we identified histones H3 and H4 as targets of the HAT regulatory properties displayed by ING1 isoforms (Figs. 4 and 5). While $p33^{ING1b}$ increased the level of acetylation of these histones, $p47^{ING1a}$ exerted the opposite effect (Figs. 4–6). Finally, we observed that these ING1-mediated HAT regulatory functions directly correlated with ING1 isoform-dependent apoptotic effects (Fig. 7).

The observations that human ING1 proteins associate with HATs (Figs. 1–3) and regulate histone acetylation (Figs. 4–6) make the biochemical basis of ING1's functions in apoptosis and the cell cycle much clearer. ING1-interacting proteins, like the HATs p300 and CBP, have been directly linked to cell cycle control and the regulation of apoptosis (38, 40, 41, 44), suggesting that the effects of ING1 on cell growth (2, 4, 22) and programmed cell death (15–20) may be due to interaction with multiple HAT, HDAC, and factor-associated acetyltransferase (FAT) complexes (24, 46). One target of ING1-induced FAT activity is the apoptotic and cell cycle regulator p53, which can physically and functionally interact with $p33^{ING1b}$ (16, 20, 21), and which is acetylated in response to elevated levels of $p33^{ING2}$ (22), another member of the ING family.

The correlations between the differential HAT and apoptotic

properties displayed by $p47^{ING1a}$ and $p33^{ING1b}$ also provide additional interpretations to help define the roles of ING1 in apoptosis and cell cycle control. By means of chromatin remodeling functions, ING1 proteins might regulate the expression of cell cycle regulators such as p21 (21), as well as survival and apoptotic genes such as Bax (22) and others (4, 22). At present it is unclear whether the effect of $p47^{ING1a}$ (Table I) is through competitive inhibition of the function of $p33^{ING1b}$ in complexes containing HAT activity, through the activation of HDAC activity, or both. Consistent with the former possibility, $p47^{ING1a}$ is clearly capable of interacting with CBP, although with considerably less avidity than $p33^{ING1b}$ (Fig. 2). Also, HDAC1 has been observed to interact in a complex with the $p33^{ING1b}$ isoform (28, 29), and we have noted that HDAC1 interacts avidly with $p47^{ING1a}$ and to a slightly lesser extent with $p33^{ING1b}$ (Fig. 3*A*).

The presence of ING1 proteins in complexes containing p300 and PCNA (Fig. 3*B*) provides additional support for a recent report linking chromatin remodeling to DNA repair through an interaction between PCNA and p300 (31), an association that was proposed to occur through an unidentified nuclear protein(s) (31). If $p33^{ING1b}$ is the protein linking PCNA with p300, overexpression of $p33^{ING1b}$ would be expected to saturate binding sites on both proteins, inhibiting the formation of complexes containing all three proteins. Such $p33^{ING1b}$-induced dissociation was seen clearly at higher levels of $p33^{ING1b}$ expression (Fig. 3). Since human (Figs. 1–3) and yeast ING1 proteins (23–25) bind to proteins present in different HAT complexes, and human ING1 proteins also seem to be involved in UV-induced cell damage responses (17, 30), the ING1 family of proteins may constitute an important link between chromatin remodeling and DNA repair. A report linking the TIP60 histone acetylase directly to DNA repair and apoptosis (43) strengthens this idea further. TIP60, a member of the MYST family of HATs, is related to the yeast Esa1 (24), which interacts with a yeast homolog of the mammalian $p33^{ING1b}$ (23). Esa1 preferentially acetylates histone H4 (24), which is also acetylated by anti-ING1 immunoprecipitates (Fig. 4).

The association observed between ING1 and CBP (Figs. 1 and 2) also helps to clarify why $p33^{ING1b}$, although a potent growth inhibitor, when overexpressed in normal cells (2), is unable to block the growth of cells expressing SV40 large T antigen (1). Since CBP is an obligate cellular target of the large T antigen oncoprotein (40) and ING1 binds CBP, the effect of ING1 in activating histone acetylation, presumably through CBP and perhaps other HAT complexes such as PCAF, would likely be neutralized.

The observations presented in this work together with previous studies suggest that ING family members exert their cellular effects through several different mechanisms related to acetylation of proteins (*e.g.* HAT, HDAC, and/or FAT activation) and that ING1 proteins could serve, based upon the degree of DNA damage, to determine whether cells undergo cell cycle arrest and DNA repair or cell cycle arrest followed by apoptosis.

Acknowledgments—We thank P. Hettiaratchi for assistance with tissue culture, D. Lane and P. Lee for anti-p53 antibodies, D. Ma for ING1 expression constructs, S. Lees-Miller for HAT assay reagents, E. Parr for insightful discussions, C. Harris and M. Nagashima for communicating data before publication, and P. Forsyth for SNB19 cells. We also thank Lori Robertson of the Faculty of Medicine FACS facility for help with flow cytometry and Donna Boland and Vanessa Berezowski of the SACRC Hybridoma Facility for immunological reagents.

REFERENCES

1. Garkavtsev, I., and Riabowol, K. (1997) *Mol. Cell. Biol.* **17,** 2014–2019
2. Garkavtsev, I., Kazarov, A., Gudkow, A., and Riabowol, K. (1996) *Nat. Genet.* **14,** 415–420
3. Cheung, K. J., Jr., and Li, G. (2001) *Exp. Cell Res.* **268,** 1–6
4. Takahashi, M., Seki, N., Ozaki, T., Kato, M., Kuno, T., Nakagawa, T., Watanabe, K., Miyazaki, Ohira, M., Hayashi, S., Hosoda, M., Tokita, H., Mizuguchi, H., Hayakawa, T., Todo, S., and Nakagawara, A. (2002) *Cancer Res.* **62,** 2203–2209
5. Garkavtsev, I., Demetrick, D., and Riabowol, K. (1997) *Cytogen. Cell Gen.* **76,** 176–178
6. Rasheed, B. K., and Bigner, S. H. (1991) *Cancer Metastasis Rev.* **10,** 289–299
7. Leonard, C., Huret, J. L., and Gfco (2002) *Bull. Cancer* **89**, 166–173
8. Ma, D., Lawless, D., and Riabowol, K. (1999) *Nat. Genet.* **23,** 373
9. Toyama, T., Iwase, H., Watson, P., Muzik, H., Saettler, E., Magliocco, A., DiFrancesco, L., Forsyth, P., Garkavtsev, I., Kobayashi, S., and Riabowol, K. (1999) *Oncogene* **18,** 5187–5193
10. Ohmori, M., Nagai, M., Tasaka, T., Koeffler, H. P., Toyama, T., Riabowol, K., and Takahara, J. (1999) *Am. J. Hematol.* **62,** 118–119
11. Jager, D., Stockert, E., Scanlan, M. J., Gure, A. O., Jager, E., Knuth, A., Old, L. J., and Chen, Y. T. (1999) *Cancer Res.* **59,** 6197–6204
12. Gunduz, M., Ouchida, M., Fukushima, K., Hanafusa, H., Etani, T., Nishioka, S., Nishizaki, K., and Shimizu, K. (2000) *Cancer Res.* **60,** 3143–3146
13. Chen, L., Matsubara, N., Yoshino, T., Nagasaka, T., Hoshizima, N., Shirakawa, Y., Naomoto, Y., Isozaki, H., Riabowol, K., and Tanaka, N. (2001) *Cancer Res.* **61,** 4345–4349
14. Sager, R. (1997) *Proc. Natl. Acad. Sci. U. S. A.* **94,** 952–955
15. Helbing, C. C., Veillette, C., Riabowol, K., Johnston, R. N., and Garkavtsev, I. (1997) *Cancer Res.* **57,** 1255–1258
16. Shinoura, N., Muramatsu, Y., Nishimura, M., Yoshida, Y., Saito, A., and Yokoyama, T., Furukawa, T., Horii, A., Hashimoto, M., Asai, A., Kirino, T., and Hamada, H. (1999) Cancer Res. **59**, 5521–5528
17. Scott, M., Bonnefin, P., Vieyra, D., Boisvert, F. M., Young, D., Bazett-Jones, D. P., and Riabowol, K. (2001) *J. Cell Sci.* **114,** 3455–3462
18. Scott, M., Boisvert, F. M., Vieyra, D., Bazett-Jones, D. P., and Riabowol, K. (2001) *Nucleic Acids Res.* **29,** 2052–2058
19. Ha, S., Lee, S., Chung, M., and Choi, Y. (2002) *Cancer Res.* **62,** 1275–1278
20. Shimada, H., Liu, T. L., Ochiai, T., Shimizu, T., Haupt, Y., Hamada, H., Abe, T., Oka, M., Takiguchi, M., and Hiwasa, T. (2002) *Oncogene* **21,** 1208–1216
21. Garkavtsev, I., Grigorian, I. A., Ossovskaya, V. S., Chernov, M. V., Chumakov, P. M., and Gudkov, A. V. (1998) *Nature* **391,** 295–298
22. Nagashima, M., Shiseki, M., Miura, K., Hagiwara, K., Linke, S. P., Pedeux, R., Wang, X. W., Yokota, J., Riabowol, K., and Harris, C. C. (2001) *Proc. Natl. Acad. Sci. U. S. A.* **98,** 9671–9676
23. Loewith, R., Meijer, M., Lees-Miller, S., Riabowol, K., and Young, D. (2000) *Mol. Cell. Biol.* **20,** 3807–3816
24. Sterner, D., and Berger, S. (2000) *Microbiol. Mol. Biol. Rev.* **64,** 435–459
25. Brown, C. E., Lechner, T., Howe, L., and Workman, J. L. (2000) *Trends Biochem. Sci.* **25,** 15–19
26. Choy, J. S., Tobe, B. T., Huh, J. H., and Kron, S. J. (2001) *J. Biol. Chem.* **276,** 43653–43662
27. Nourani, A., Doyon, Y., Utley, R. T., Allard, S., Lane, W. S., and Cote, J. (2001) *Mol. Cell. Biol.* **21,** 7629–7640
28. Skowyra, D., Zeremski, M., Neznanov, N., Li, M., Choi, Y, Uesugi, M., Hauser, C. A., Gu, W., Gudkov, A., and Qin, J. (2001) *J. Biol. Chem.* **276,** 8734–8739
29. Kuzmichev, A., Zhang, Y., Erdjument-Bromage, H., Tempst, P., and Reinberg, D. (2002) *Mol. Cell. Biol.* **22,** 835–848
30. Cheung, K.-J., Jr., Mitchell, D., Lin, P., and Li, G. (2001) *Cancer Res.* **61,** 4974–4977
31. Hasan, S., Hassa, P. O., Imhof, R., and Hottiger, M. O. (2001) *Nature* **410,** 387–391
32. McMahon, S. B., Wood, M. A., and Cole, M. C. (2000) *Mol. Cell. Biol.* **20,** 556–562
33. McMahon, S. B., Van Buskirk, H. A., Dugan, K. A., Copeland, T. D., and Cole, M. D. (1998) *Cell* **94,** 363–374
34. Garkavtsev, I., Boland, D., Mai, J., Wilson, H., Veillette, C., and Riabowol, K. (1997) *Hybridoma* **16,** 537–540
35. Boland, D., Olineck, V., Bonnefin, P., Vieyra, D., Parr, E., and Riabowol, K. (2000) *Hybridoma* **19,** 161–165
36. Riabowol, K., Schiff, J., and Gilman, M. (1992) *Proc. Natl. Acad. Sci. U. S. A.* **89,** 157–161
37. Riabowol, K. T., Draetta, G., Brizuela, L., Vendre, D., and Beach, D. (1989) *Cell* **57,** 393–401
38. Yang, X.-J., Ogryzko, V., Nishikawa, J., Hpward, B., and Nakatani, Y. (1996) *Nature* **382,** 319–324
39. Ogryzko, V. V., Schiltz, R. L., Russanova, V., Howard, B. H., and Nakatani, Y. (1996) *Cell* **87,** 953–959
40. Eckner, R., Ludlow, J. W., Lill, N. L., Oldread, E., Arany, Z., Modjtahedi, N., DeCaprio, J. A., Livingston, D. M., and Morgan, J. A. (1996) *Mol. Cell. Biol.* **16,** 3454–3464
41. Bannister, A. J., and Kouzarides, T. (1995) *EMBO J.* **14,** 4758–4762
42. Hague, A., Manning, A. M., Hanlon, K. A., Huschtscha, L. I., Hart, D., and Paraskeva, C. (1993) *Int. J. Cancer* **55,** 498–505
43. Ikura, T., Ogryzko, V. V., Grigoriev, M., Groisman, R., Wang, J., Horikoshi, M., Scully, R., Qin, J., and Nakatani, Y. (2000) *Cell* **102,** 463–473
44. Kung, A. L., Rebel, V. I., Bronson, R. T., Ch'ng, L. E., Sieff, C. A., Livingston, D. M., and Yao, T. P. (2000) Genes Dev. **14**, 272–277
45. Giordano, A., and Avantaggiati, M. (1999) *J. Cell. Physiol.* **181,** 218–230
46. Fryer, C., and Archer, T. (1998) *Nature* **393,** 88–91